

All Stabilizing State Feedback Controller for Inverted Pendulum Mechanism

Rahman Bitirgen* Muhsin Hancer** Ismail Bayezit*

* Faculty of Aeronautics and Astronautics, Istanbul Technical University, Istanbul, Turkey (e-mail: bitirgen@itu.edu.tr, bayezit@itu.edu.tr)

** Faculty of Aeronautical and Space Sciences, Necmettin Erbakan University, Konya, Turkey (e-mail: mhancer@konya.edu.tr)

Abstract: In the literature, finding all stabilizing controllers are widely studied. In this paper, a case study of inverted pendulum is considered to test the methods for finding stabilizing state feedback controller. First, good set of state feedback gain matrix is calculated, two of feedback parameters are fixed to reduce the computational cost. The other two of feedback parameters that make the system stable are then calculated by gridding. The boundary of the stability region is calculated with the frequency method. In order to have fast response, the eigenvalue region of the closed loop system is defined as the left hand side of the $-1 + j\omega$ line and the stability region for feedback gains are calculated for this scenario.

Keywords: all stabilizing controller, full state feedback, PID controller, inverted pendulum, stability region, actuator saturation

1. INTRODUCTION

In the literature, rather than finding a good set of controller for a given system, the topic of finding all stabilizing PID controller is studied by many researchers. In order to test these possible controllers, inverted pendulum has widely used by many researchers as a useful testbed Yadav et al. (2016). Inverted pendulum also has parametric uncertainties in both model parameters and designing controllers or compensator Yue et al. (2015).

A certain set of performance criteria is optimized in Malan et al. (1994), Saeki and Kimura (1997), Ohta et al. (1997), Daley and Liu (1999). But this optimization decreases the uncalculated or unexpected performance loss. So, finding all stabilizing PID controllers to design controller is helpful. In this context, Shafiei and Shenton (1994) and Shafiei and Shenton (1997) have proposed a graphical approach using D-partitioning method to determine the borders of absolute and relative stability regions in the parameter space. Characterization of all the stabilizing gains using a generalized Hermite-Biehler theorem is provided in Ho et al. (1996). Then, Ho et al. (1997b) and Ho et al. (1997a) have extended this results to characterize stabilizing PID compensators. Ho et al. (1998) found a systematic way of finding the maximum and minimum values of the K_p , K_i , and K_d terms to guarantee stability in the resulting closed-loop system based on generalization of the Hermite-Biehler Theorem. Munro (1999) proposed a new method to this problem based on the use of the Nyquist plot.

Munro and Soylemez (2000) claimed that Nyquist plot based approach is computationally much faster than that of Ho et al. (1998) and Shafiei and Shenton (1997), and the computing time is polynomial with system order, it was recently realized that for systems with no explicit

time delay term, or for situations where time delay could be adequately represented by a Padé approximation, a simpler approach to this problem could be implemented by Munro (1999) and Munro et al. (1999).

Munro (1999) and Munro et al. (1999) suggested a numerical frequency domain approach in order to find the set of D-stabilizing low-order compensators. Datta et al. (2013), Ackermann and Kaesbauer (2001), and Bajcinca (2006) have shown that the stabilizing region is defined by a set of convex polygonal slices normal to K_p axis in the $(K_p, K_i, \text{ and } K_d)$ parameter space for continuous time PID controllers.

In this paper, the Quanser inverted pendulum platform is taken as a case study. The rest of the paper is organized as follows. In Section 2, the mathematical model is given and nonlinearities such as trigonometric terms are eliminated with the help of linearization. The parameters of the system is assumed to be certain and obtained with measurements and with identification test cycles. The controllability and observability of the system is tested. In section 3, firstly, full state feedback controller is proposed in PD based with instant measurement of displacement, speed, angle, and angular rate. The system has four states and therefore the controller has four parameters. Finding all stabilizing state feedback controllers requires searching for all four parameters at the same time, so a constraint is introduced, two of its parameters are fixed and the stabilizing region for the other two are calculated by gridding and frequency methods. A gain is then chosen to test the response of the system, due to actuator saturation, the system is close to instability. To overcome this situation, the gain K is searched which makes all the roots stay on the left hand side of $-1 + j\omega$ axis. Then a test point is chosen and results are presented in section 4.

2. SINGLE INVERTED PENDULUM PLATFORM

Inverted pendulum with moving cart mechanism is a widely-used platform to test new approaches in controller design. Pendulum with moving cart on a track has two equilibrium points: first, pendulum aligned with the gravity vector pointing downwards, the other is pendulum being again aligned with the gravity vector and in this case pointing upwards. The first equilibrium point is inherently stable because the center of the gravity (CG) of the pendulum is below the pivot point. In the second equilibrium point, the CG of the pendulum is above the pivot point and marginally unstable. Therefore the pendulum diverges and return the asymptotic stability condition when it is disturbed with an insignificant force or moment. The second condition is marginally unstable due to this behaviour, controllers often implemented to make the system stable in the inverted configuration.

In Fig. 1 and 2 the testbed configuration can be seen. The cart can move left and right on the track, and the pendulum can rotate around the pivot axis. This testbed is a Single-Input Multiple-Output (SIMO) system, one input is the motor voltage and two outputs are the position of the cart and the pendulum angle. It has two high resolution encoders to measure the displacement of the cart and the pendulum angle. There is a DC motor to move the cart along the track which is the actuator to control the system.

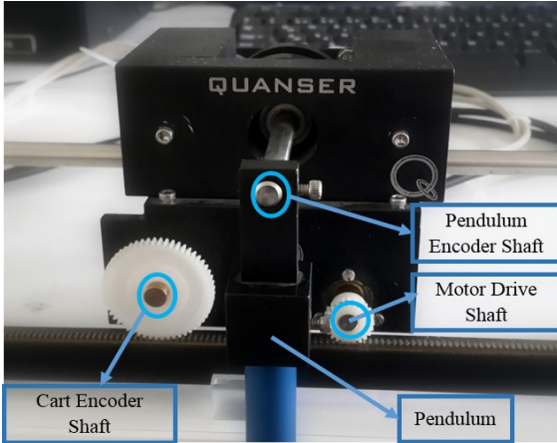


Fig. 1. Pendulum on a moving cart test platform.

2.1 Mathematical Model

The mathematical model of the system is derived from the Newton's second law of motion. The equations are nonlinear and needs to be linearized in order to design linear controller. Assuming that the angle of the pendulum is small, the equations are linearized.

$$\begin{aligned} \ddot{x}_c &= \frac{1}{J_T} (-J_\kappa B_{eq} \dot{x}_c - M_p l_p B_p \dot{\alpha} + M_p^2 l_p^2 g \alpha + J_\kappa F_c) \\ \ddot{\alpha} &= \frac{1}{J_T} (- (M_p l_p B_{eq}) \dot{x}_c - J_\xi B_p \dot{\alpha} + J_\xi M_p l_p g \alpha + M_p l_p F_c) \end{aligned} \quad (1)$$

where

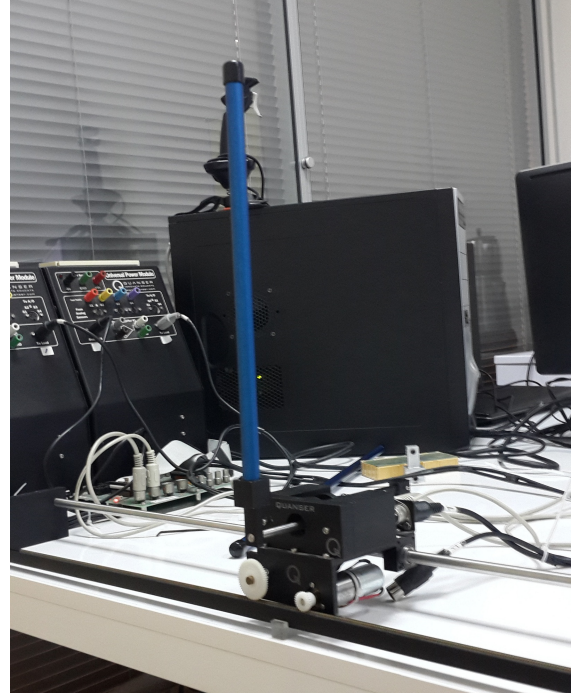


Fig. 2. Inverted Pendulum Platform

$$\begin{aligned} J_{eq} &= M_c + \frac{\eta_g K_g^2 J_m}{r_{mp}^2} \\ J_T &= J_{eq} J_p + M_p J_p + J_{eq} M_p l_p^2 \\ J_\kappa &= J_p + M_p l_p^2 \\ J_\xi &= J_{eq} + M_p \end{aligned} \quad (2)$$

2.2 State Space Form

The system can be represented in state space format. The state vector:

$$x = [x_c \ \alpha \ \dot{x}_c \ \dot{\alpha}]^T \quad (3)$$

The state space representation:

$$\begin{aligned} \dot{x} &= Ax + Bu \\ y &= Cx + Du \end{aligned} \quad (4)$$

where x_c is the position of the cart, \dot{x}_c is the speed of the cart, α is the pendulum angle, $\dot{\alpha}$ is the pendulum angular rate and u is the control signal which is voltage on the motor. The system matrix:

$$A = \frac{1}{J_T} \begin{bmatrix} 0 & 0 & 1 & 0 \\ 0 & 0 & 0 & 1 \\ 0 & M_p^2 l_p^2 g & -J_\kappa B_{eq} & -M_p l_p B_p \\ 0 & J_\xi M_p l_p g & -M_p l_p B_{eq} & -J_\xi B_p \end{bmatrix} \quad (5)$$

$$B = \frac{1}{J_T} [0 \ 0 \ J_\kappa \ M_p l_p]^T \quad (6)$$

$$C = \begin{bmatrix} 1 & 0 & 0 & 0 \\ 0 & 1 & 0 & 0 \end{bmatrix} \quad (7)$$

$$D = \begin{bmatrix} 0 & 0 \\ 0 & 0 \end{bmatrix} \quad (8)$$

Here in the equations, $M_p = 0.127(kg)$ is the mass of the pendulum, $J_p = 1.19 * 10^{-3}(kg/m^2)$, is the mass moment of inertia of the pendulum about its center of gravity, $l_p = 0.178(m)$ is the distance from the center of gravity of the pendulum to the pivot point, g is the gravitational acceleration, $B_{eq} = 5.4(Ns/m)$ is the friction coefficient between the cart and the track, $B_p = 2.4 * 10^{-3}(Nms/rad)$, is the viscous damping coefficient at the pendulum axis, $M_c = 0.57(kg)$ is the mass of the cart, $\eta_g = 1$ is the planetary gearbox efficiency, $K_g = 3.71$ is the planetary gearbox gear ratio, $J_m = 3.90 * 10^{-7}(kgm^2)$ rotor inertia, $r_{mp} = 6.35 * 10^{-3}(m)$ is the motor pinion radius. The terms J_{eq} , J_T , J_κ and J_ξ are related to inertias, can be calculated with the given parameters.

The poles of the open loop system:

$$P = [0 \ 6.38 \ -6.38 \ -12.47] \quad (9)$$

There is a pole on the right hand side of the s plane for the open loop system, therefore it is proved that the open loop system is unstable.

Controllability and observability are checked before designing the controller, in order to inspect if all modes are controllable and if all the states are observable. The controllability matrix is calculated and it is seen that it does not lose rank therefore the system is controllable.

The observability matrix does not lose rank, therefore it is possible to observe all the states.

3. CONTROLLER DESIGN

The system has one input and two outputs, and therefore it can be represented with two transfer functions. However, when PID controller is designed for each of the transfer function (TF) assuming each TF has a SISO behaviour, the control input for each controller only takes into account the position or the angle feedback individually. This make it difficult to find a set of controller that both satisfies the stability of position and angle. It is considered that, with a full state-feedback controller, all poles of the system can be placed anywhere in the left half plane to make the system stable.

$$u = -Kx \quad K = [k_1 \ k_2 \ k_3 \ k_4] \quad x = [x_c \ \alpha \ \dot{x}_c \ \dot{\alpha}]^T \quad (10)$$

It should be noted that, k_1 and k_3 behaves like a Proportional-Derivative (PD) controller for the position of the cart, and k_2, k_4 pair behaves like a PD controller for the pendulum angle. Pole placement method can be used to find the stabilizing K when desired location of the closed loop system poles are known. In this case, it is known by both simulation and experiment on the actual system, poles in (11) stabilizes the system.

$$P = [-2 \ -3 \ -18 + 10j \ -18 - 10j]^T \quad (11)$$

The closed loop system matrix:

$$A_c = A - BK \quad (12)$$

The desired poles of the closed loop system is given, and by solving Ackermann's formula, one can calculate the gain K . In this case, K is calculated as:

$$K = [-42 \ 115 \ -46 \ 15] \quad (13)$$

In this paper, a good set of K value is calculated, then it is to be found when k_1 and k_3 (the part of the K that controls the position and velocity of the cart.) are fixed, what are the possible sets of k_2 and k_4 (the part of the K that controls the angle and angular velocity of the pendulum.). Two methods are used to find all possible values of k_2 and k_4 .

3.1 Gridding Method

In this brute force method, k_2 and k_4 are gridded between the values of 0 and 250. k_1 and k_3 are fixed, for each and every single point on the grid, it is possible to calculate the roots of the characteristic equation. If the point on the grid does not have any root on the right half plane, then that K is said to be possible stabilizing controller for the system. When the gridding is dense enough, this method can give all possible K that stabilizes the system when k_1 and k_3 are fixed. However, it should be noted that this is a computationally expensive method, when the gridding is dense, it takes time to give a solution.

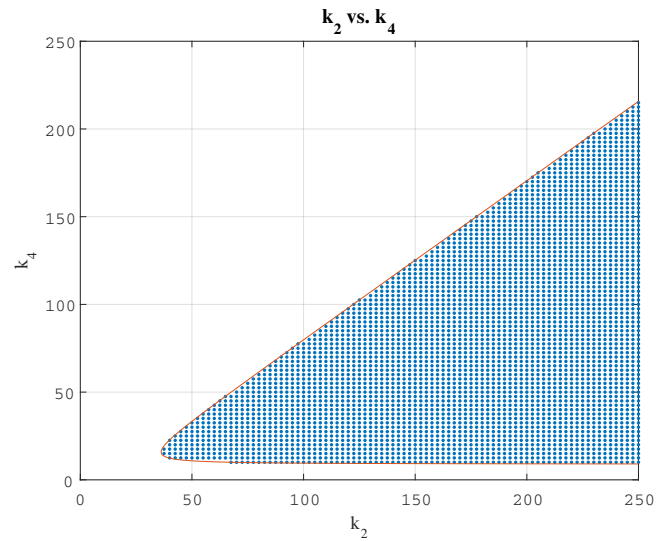


Fig. 3. All Possible Stabilizing Values of k_2 and k_4 when $k_1 = -42$ and $k_3 = -46$

3.2 Frequency Method

In Fig. 3, it can be seen that the 2D shape have boundaries. On the stable side of the boundary, if a k_2 and k_4 pair is chosen and roots are calculated, the roots are observed to be close to the imaginary axis on the left half plane, when on the border, two roots of the system are on the imaginary axis.

In this sense, it can be computationally less expensive to search the boundaries of the stabilizing k_2 and k_4 . Instead of s in the characteristic equation, $j\omega$ is placed. Now in this case, k_2 and k_4 are not gridded and are to be found. In order for $j\omega$ to be a root of the characteristic equation, real and imaginary part of the $P_c(j\omega)$ should be equal to

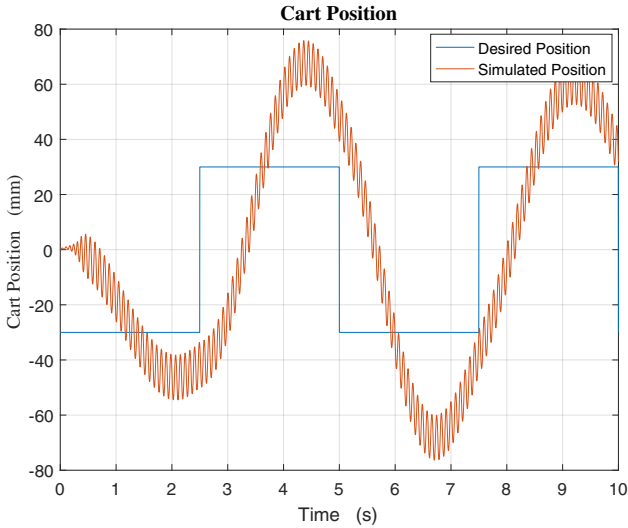


Fig. 4. Cart Position Time Response for $K = [-42 \ 180 \ -46 \ 50]$

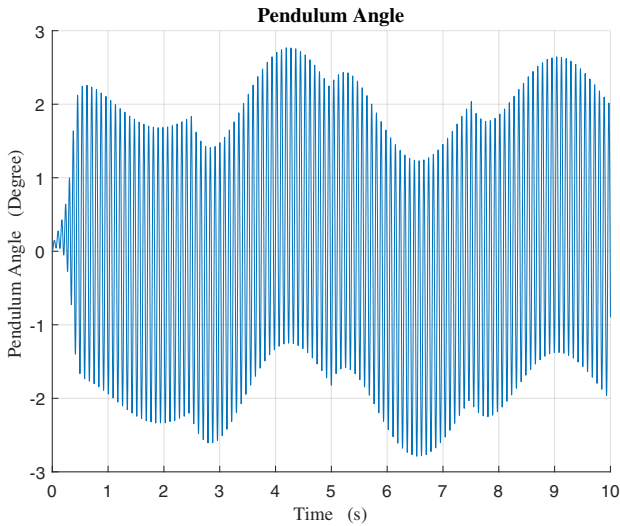


Fig. 5. Pendulum Angle Time Response for $K = [-42 \ 180 \ -46 \ 50]$

zero. There comes two equations, one from the real part, and one from the imaginary part. There are two unknowns and two equations, thus k_2 and k_4 can be calculated given ω .

In this method, only ω is gridded, and no root calculations are done, only two linear equations are solved to find k_2 and k_4 . It can be said that, this method, comparing it to the gridding method is computationally less expensive. However, in this method, only the boundaries are calculated and it is not known which side of the boundary is stable. In this case a test set can be chosen to test whether the region is stable or not.

Placing $j\omega$ instead of s in the characteristic equation:

$$\begin{aligned} P_c(s) &= a_4 s^4 + a_3 s^3 + a_2 s^2 + a_1 s + a_0 \\ P_c(j\omega) &= a_4 \omega^4 - a_3 \omega^3 j - a_2 \omega^2 + a_1 \omega j + a_0 \end{aligned} \quad (14)$$

where

$$\begin{aligned} a_4 &= 1 \\ a_3 &= 1.56k_3 + 6.78k_4 + 12.42 \\ a_2 &= 1.56k_1 + 6.78k_2 + 0.72k_3 - 40.77 \\ a_1 &= -66.45k_1 \end{aligned} \quad (15)$$

In order for $j\omega$ to be a root of the characteristic equation, both real and imaginary parts of the $P_c(j\omega)$ should be equal to zero.

$$\begin{aligned} Re\{P_c(s)\} &= a_4 \omega^4 - a_2 \omega^2 + a_0 = 0 \\ Im\{P_c(s)\} &= -\omega (a_3 \omega^2 - a_1 \omega) = 0 \end{aligned} \quad (16)$$

Solving (16) for k_2 and k_4 :

$$\begin{aligned} k_2 &= \frac{\omega^4 - b_1(k_1, k_3)\omega^2 + b_2(k_1)}{b_3\omega^2} \\ k_4 &= \frac{-c_1(k_3)\omega^2 + c_2(k_1, k_3)}{c_3\omega^2} \end{aligned} \quad (17)$$

where

$$\begin{aligned} b_1 &= 1.56k_1 + 0.72k_3 - 40.77 \\ b_2 &= -66.45k_1 \\ b_3 &= 6.78 \\ c_1 &= 1.56k_3 + 12.42 \\ c_2 &= 0.72k_1 - 66.54k_3 - 506.64 \\ c_3 &= 6.78 \end{aligned} \quad (18)$$

First limit values of k_2 and k_4 are calculated, when $\omega = 0$ and $\omega \rightarrow \infty$. In order to calculate k_2 and k_4 only ω is gridded between frequencies 0 and 1000.

Table 1. Limit Values for k_2 and k_4

ω	k_2	k_4
0	∞	∞
∞	∞	$-\frac{c_1}{c_3}$

In Fig. 3 the blue dots are calculated with the gridding method, and the red curve is the boundary calculated by the frequency method. In this figure, any value of k_2 and k_4 in the stability region makes the system stable theoretically. A set of K is chosen and implemented in the simulation, the results are presented in the Fig. 4 for cart position, Fig. 5 for pendulum angle. These figures inspire the control system engineer to revise the controller gains, in order to mitigate high oscillation rates and prevent actuator saturation.

The stability boundary $j\omega$ could be shifted to further left $-1 + j\omega$ to avoid such situations, in this case, any K set that have at least one root between $j\omega$ and $-1 + j\omega$ lines are disregarded.

In the gridding method, K values that make the closed loop system to have roots on the left hand side of $-1 + j\omega$ are taken into the new stability region, and for the frequency method, $-1 + j\omega$ is placed instead of s in the characteristic equation. The same approach is then used to calculate the stability boundary via gridding the frequency.

In Fig. 6, the blue dots are the k_2 and k_4 pairs that are calculated with the gridding method. The red curve is the $j\omega$ crossing values of k_2 and k_4 and the orange curve is the $-1 + j\omega$ crossing values for k_2 and k_4 .

It can be observed that the new stability region is significantly smaller comparing it to Hurwitz stability and it is also a bounded region.

An arbitrary pair is chosen in this region.

$$K = [-42 \ 145 \ -46 \ 25]$$

The experiment is conducted on the actual system and the results are presented in the Figs. 8, 9 and 10. The time responses of cart position, pendulum angle and motor voltage are better comparing it to the first case scenario. It can be noticed that, for the cart position, there is a steady state error. This is due to the fact that the mathematical model of the system does not represent the system exactly. In the mathematical model, the cart can move very small distances, however in the real system there is contact between the cart and the track and the minimum distance that the cart can travel depend on the dimension of the gears. Therefore, when the cart and pendulum settles on a point on the track, the amount of control signal that comes from the feedback of position and speed, is not enough to change the position. Because, at the same time, the feedback from the angle and angular rate also act to stabilize the pendulum in the upward configuration. This can be eliminated with introducing an integral term for the position part of the controller.

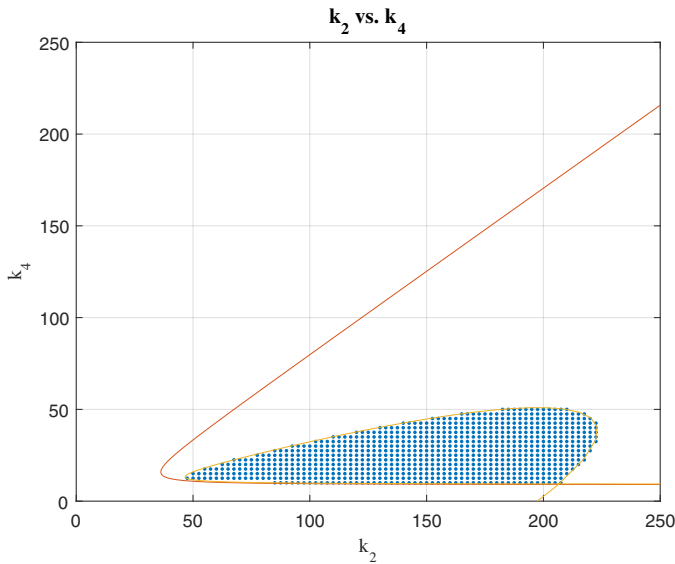


Fig. 6. Values of k_2 and k_4 when $k_1 = -42$ and $k_3 = -46$ that places the poles on the left side of $-1 + j\omega$

4. CONCLUSIONS

In this paper, a well-known test-bed is used to test methods to find all possible controllers when two of its parameters are fixed. The stability region for the other two parameters are calculated using two different methods,

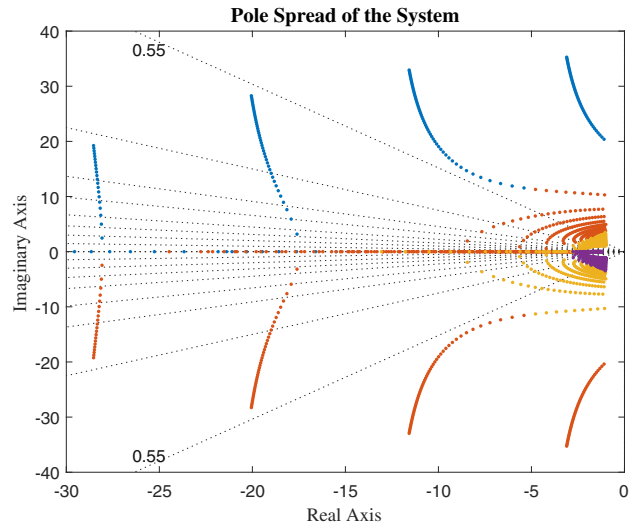


Fig. 7. Pole Spread of the system when controller is within the boundaries of the stability region shown in Fig. 6

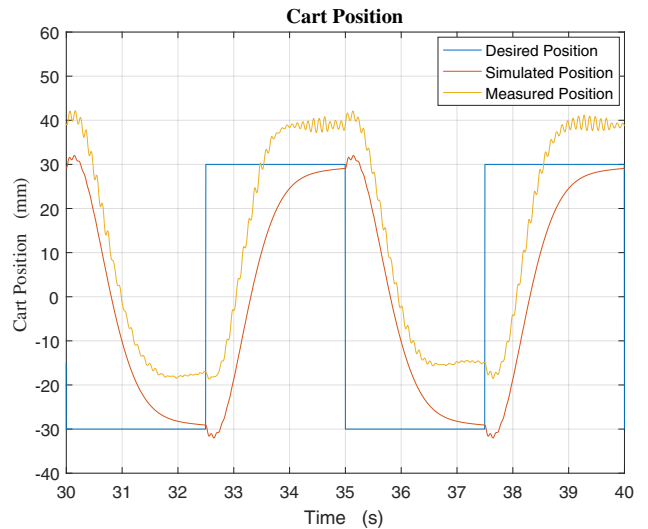


Fig. 8. Cart Position Time Response for $K = [-42 \ 145 \ -46 \ 25]$

namely gridding and frequency methods. The latter is observed to be less computationally expensive comparing the first method.

Considering only Hurwitz stability, the stability region for k_2 and k_4 might have some values of K that cannot drive the system to stability because of unmodelled dynamics and actuator saturation. In order to overcome this situation, the stability boundary is taken as the left half side of $-1 + j\omega$ line. Taking an arbitrary point from this region, the system is driven to stability without actuator saturation.

For future research, the authors plan to take the friction coefficient as an uncertain parameter and then calculate all stabilizing gains when the exact value of the parameter is unknown but is bounded. The length of the pendulum can also be taken as an uncertain parameter, however in this case this uncertain parameter enters in the characteristic equation, polynomial fractional fashion. It can also be

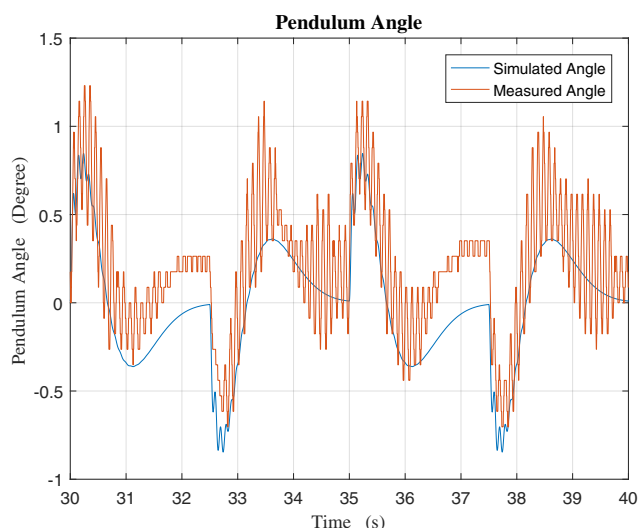


Fig. 9. Pendulum Angle Time Response for $K = [-42 \ 145 \ -46 \ 25]$

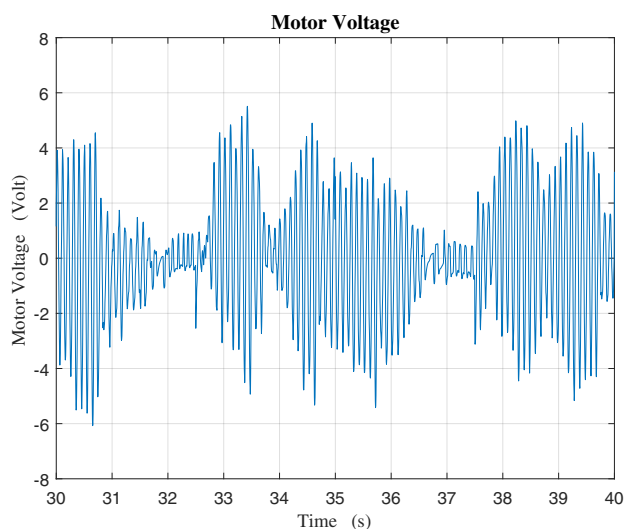


Fig. 10. Motor Voltage Time Response for $K = [-42 \ 145 \ -46 \ 25]$

studied on the steady state error of the cart position by adding an integral term in K .

ACKNOWLEDGEMENTS

The authors would like to thank to the BAP (Scientific Research Projects) Office of ITU for funding the laboratory.

The authors also would like to thank Prof. M. Turan Söylemez for providing vision throughout the entire course of Control of System with Parametric Uncertainty during Fall Term of 2017-2018.

REFERENCES

Ackermann, J. and Kaesbauer, D. (2001). Design of robust pid controllers. In *Control Conference (ECC), 2001 European*, 522–527. IEEE.

Bajcinca, N. (2006). Design of robust pid controllers using decoupling at singular frequencies. *Automatica*, 42(11), 1943–1949.

Daley, S. and Liu, G. (1999). Optimal pid tuning using direct search algorithms. *Computing & Control Engineering Journal*, 10(2), 51–56.

Datta, A., Ho, M.T., and Bhattacharyya, S.P. (2013). *Structure and synthesis of PID controllers*. Springer Science & Business Media.

Ho, M.T., Datta, A., and Bhattacharyya, S. (1996). A new approach to feedback stabilization. In *Decision and Control, 1996., Proceedings of the 35th IEEE Conference on*, volume 4, 4643–4648. IEEE.

Ho, M.T., Datta, A., and Bhattacharyya, S. (1997a). Control system design using low order controllers: constant gain, pi and pid. In *American Control Conference, 1997. Proceedings of the 1997*, volume 1, 571–578. IEEE.

Ho, M.T., Datta, A., and Bhattacharyya, S. (1997b). A linear programming characterization of all stabilizing pid controllers. In *American Control Conference, 1997. Proceedings of the 1997*, volume 6, 3922–3928. IEEE.

Ho, M.T., Datta, A., and Bhattacharyya, S. (1998). Design of p, pi and pid controllers for interval plants. In *American Control Conference, 1998. Proceedings of the 1998*, volume 4, 2496–2501. IEEE.

Malan, S.A., Milanese, M., and Taragna, M. (1994). Robust tuning for pid controllers with multiple performance specifications. In *Decision and Control, 1994., Proceedings of the 33rd IEEE Conference on*, volume 3, 2684–2689. IEEE.

Munro, N. and Soylemez, M. (2000). Fast calculation of stabilizing pid controllers for uncertain parameter systems. *IFAC Proceedings Volumes*, 33(14), 549–554.

Munro, N., Söylemez, M., and Baki, H. (1999). Computation of d-stabilizing low-order compensators. *Control Systems Centre Report*, 882.

Munro, N. (1999). The systematic design of pid controllers.

Ohta, Y., Li, J., Tagawa, K., and Haneda, H. (1997). Robust pid controller design. In *Proceedings of NOLTA*, 1053–1056.

Saeki, M. and Kimura, J. (1997). Design method of robust pid controller and cad system. *IFAC Proceedings Volumes*, 30(11), 1511–1516.

Shafiei, Z. and Shenton, A. (1994). Tuning of pid-type controllers for stable and unstable systems with time delay. *Automatica*, 30(10), 1609–1615.

Shafiei, Z. and Shenton, A. (1997). Frequency-domain design of pid controllers for stable and unstable systems with time delay. *Automatica*, 33(12), 2223–2232.

Yadav, M., Gupta, A.K., Pratap, B., and Saini, S. (2016). Robust control design for inverted pendulum system with uncertain disturbances. In *Power Electronics, Intelligent Control and Energy Systems (ICPEICES), IEEE International Conference on*, 1–6. IEEE.

Yue, M., Wei, X., and Li, Z. (2015). Zero-dynamics-based adaptive sliding mode control for a wheeled inverted pendulum with parametric friction and uncertain dynamics compensation. *Transactions of the Institute of Measurement and Control*, 37(1), 91–99.